Supporting Information

Indolo[3,2-b]carbazole-based MOF for oxidative coupling of amines powered by blue light

Chao Wei[a,b], Si-Jia Wang[a], Ji-Wei Li[a], Fan Li[a], Zhou-Rui Yan[a], Ming Lu[a], Xiao-Qin Liu[a], Guoliang Liu[a*], and Lin-Bing Sun[a*]

[a] State Key Laboratory of Materials-Oriented Chemical Engineering, Jiangsu National Synergetic Innovation Center for Advanced Materials (SICAM), College of Chemical Engineering, Nanjing Tech University, Nanjing 211816, China

[b] College of Science, Jinling Institute of Technology, Nanjing 211169, China

* Corresponding authors. E-mail: glliu@njtech.edu.cn; lbsun@njtech.edu.cn

General information

Chemicals and reagents

4-Formylbenzoic acid (99%+, Aladdin), indole-6-carboxylic acid (98%+, Adamas), tetrabutylammonium iodide (99%+, Aladdin), zinc nitrate hexahydrate ($Zn(NO_3)_2$ $6H_2O$, Sigma-Aldrich), benzylamine and its derivatives (Adamas, 99%), HBF_4 (48%, Sigma-Aldrich), iodine (I_2, Adamas, 99%), deuterated dimethyl sulfoxide (Adamas, 99.9%D+0.03%TMS) were purchased from corresponding suppliers. 37% HCl (99%, Adamas), methanol (MeOH), N, N-dimethylformamide (DMF), acetonitrile (MeCN), ethanol (EtOH), 5,5-dimethyl-1-pyrroline Noxide (DMPO), 2,2,6,6-tetramethylpiperidine (TEMP) and deionized water were purchased as the reagent grade from Sinopharm Chemical Reagent Shanghai Co., Ltd. and 420 nm LED (45 W, from Xuzhou Aijia Electrical Technology) were used for irradiation.

Instrumentations for characterizations

^1H NMR and ^{13}C NMR spectra were recorded at room temperature on a Bruker Avance 400 MHz spectrometer. Chemical shifts are given in ppm with respect to TMS. Fourier transform infrared (FT-IR) spectra were recorded on KBr (1:30, w/w) pellets in the 4000-600 cm^{-1} range using a Perkin-Elmer Spectrum Two FT-IR spectrometer. Powder X-ray diffraction (PXRD) data were collected at 40 kV and 200 mA on a SmartLab 9kW X-Ray diffractometer using Cu-Kα radiation (λ = 1.5418 Å) over 2θ range of 5.0 °-30 ° at room temperature. Thermogravimetric analyses (TGA) were obtained on a Netzsch TG 209 TG-DTA analyzer with a heating rate of 10 ℃·min^{-1} under N_2 flow (60 mL/min) from room temperature to 800 ℃. N_2 adsorption-desorption isotherms were carried out employing BELSORP-MAX analyzer at 77 K. The Brunauer-Emmett-Teller (BET) surface area was calculated using adsorption data in a relative pressure ranging from 0.05 to 0.30. The pore diameter was calculated from the adsorption branch by using the no-local density functional theory (NLDFT) method. UV-vis spectra were obtained on a Shimadzu UV-2600i spectrophotometer and the test range is from 200 to 800 nm. Samples were treated via Pt sputtering before observation. Photoluminescence (PL) emission spectra of the samples were collected on a Perkin-Elmer Spectrum FL 6500 fluorescence

spectrophotometer at room temperature. The blue LED (430 nm, 45 W) employed in the photocatalytic experiments has an irradiation area of 15 cm^2 and a power density of about 120 mW/cm^2. The electron paramagnetic resonance (EPR) experiments were conducted on an electron paramagnetic resonance spectrometer (JEOL, JES-FA300). Single crystal X-ray diffraction analysis was collected on a Bruker APEX-II CCD diffractometer with graphite-monochromated Cu Kα radiation (λ = 1.54178). Its scanning method is ϕ/ω, the structure is analyzed by the direct method, and refined on F^2 by the SHELXTL program. The reflection data were corrected by using the SADABS program. Applied anisotropic thermal parameters to non-hydrogen atoms, all hydrogen atoms in organic ligands were counted and added to ideal positions. Due to the inability to identify solvents and ions located in the voids. Therefore, perform SQUEEZE in the PLATON program to remove highly disordered solvents and ions. The relevant crystallographic data were shown in Table S1. Selected bond lengths and angles were listed in Table S2. The CCDC numbers were 2506010 and 2506011 for H_4BAICz and NUT-121, respectively.

EPR experiment

For the detection of $O_2^{\bullet-}$, 0.1 mL of DMPO/DMF solution (30 uL/1.0 mL) was mixed with 1.0 mL of NUT-121/DMF (3.0 mg/1.0 mL), which was irradiated with a 45 W blue LEDs for 15 min at room temperature under air atmosphere, then separating the filtrate with a 0.9 mm capillary tube transferred to EPR (electron paramagnetic resonance) tube for measurements. The detection of $^1O_2$ was conducted, employing a similar process but utilizing TEMP as the trapping agent.

Additional figures and tables

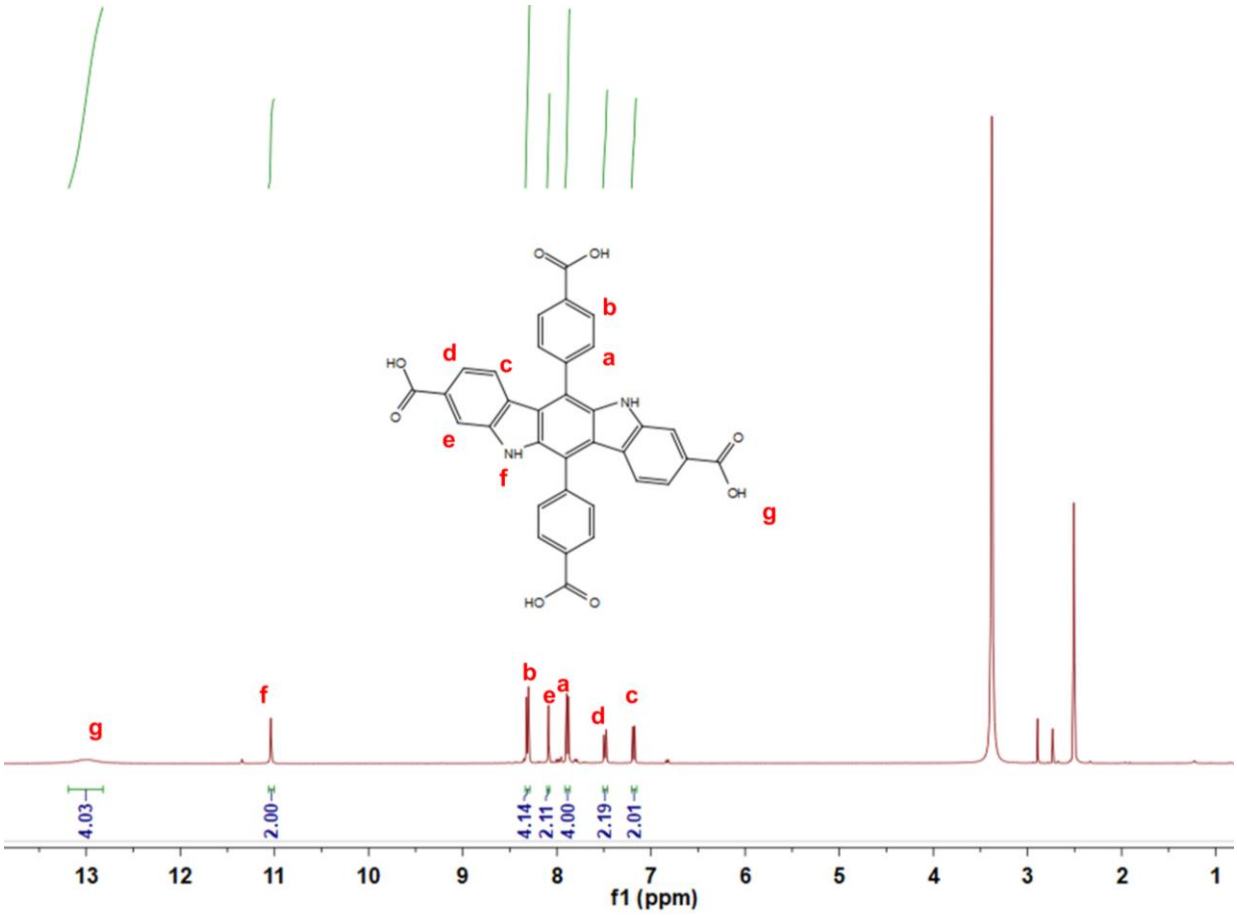

Fig. S1 ^{1}H NMR spectrum of H_4BAICz.

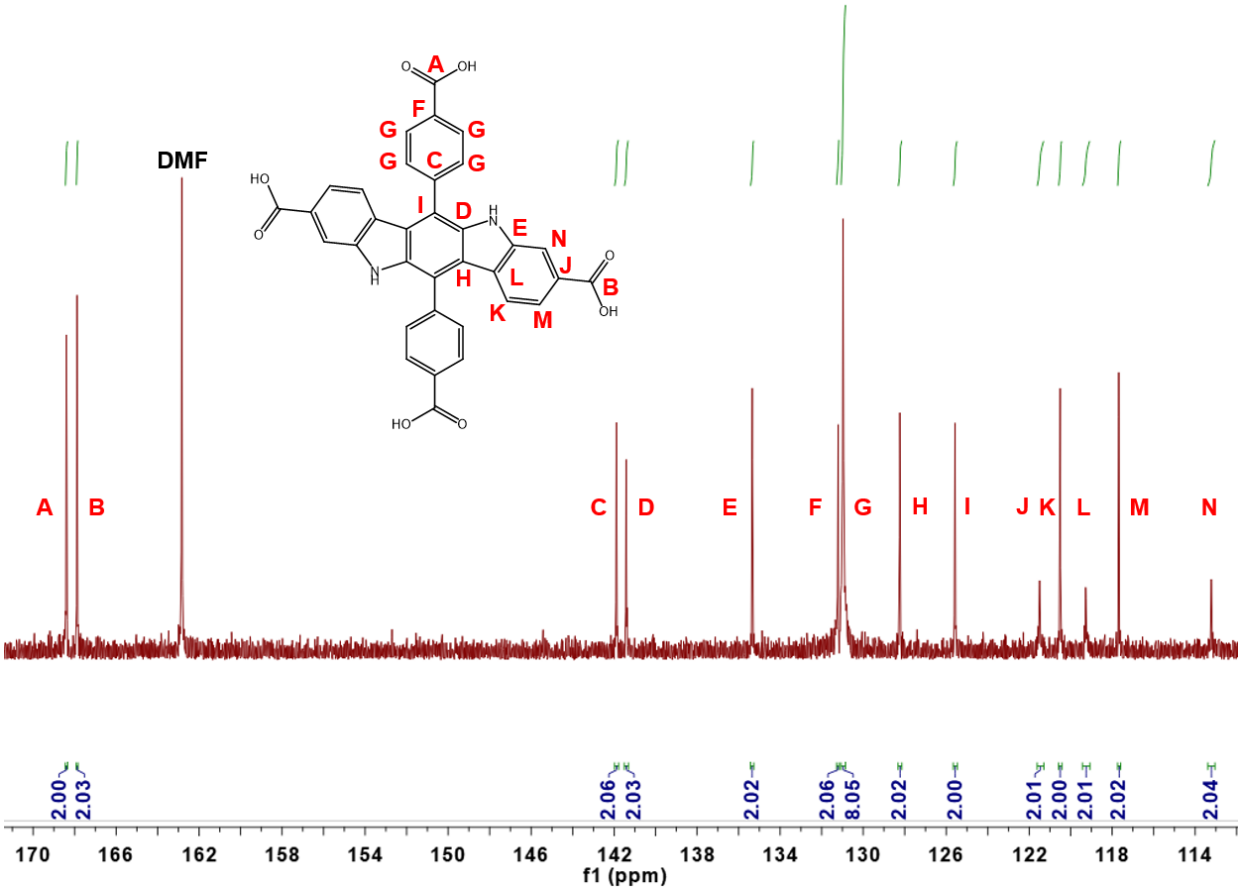

Fig. S2 ^{13}C NMR spectrum of H_4BAICz.

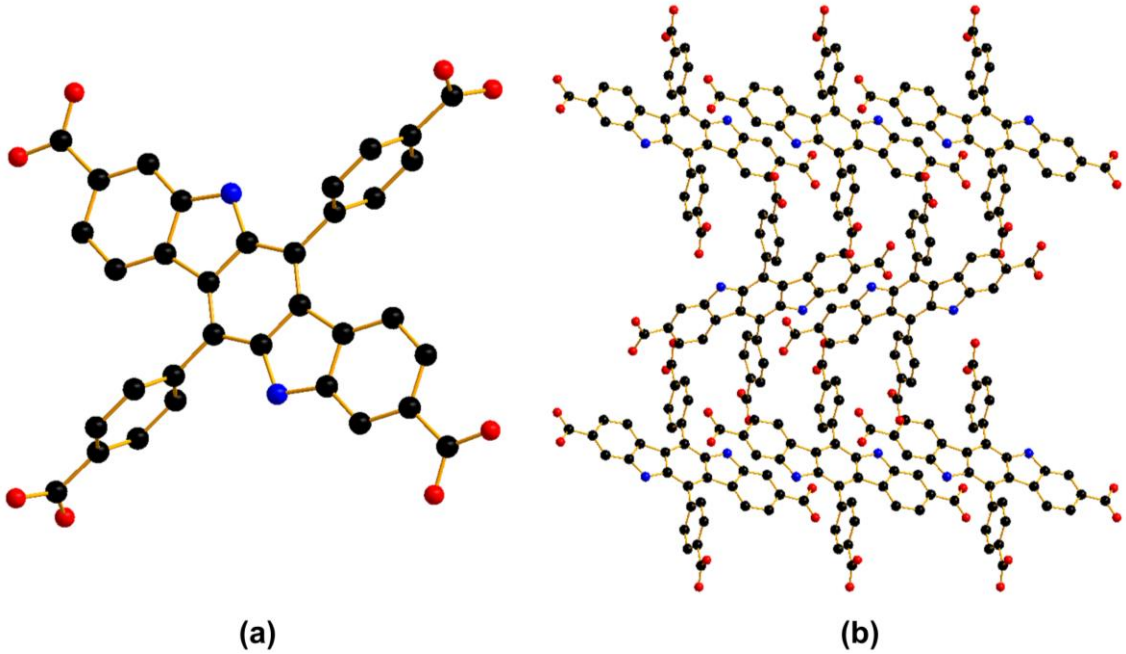

Fig. S3 (a) Structure of H_4BAICz and (b) stacking diagram of H_4BAICz (H atoms are omitted for clarity).

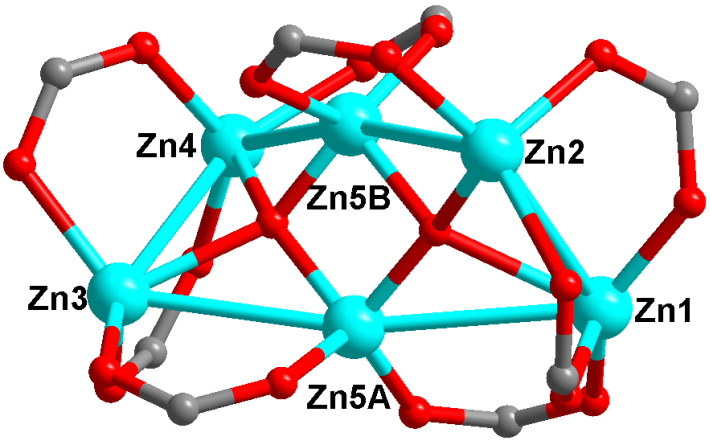

Fig. S4 The Zn cluster of NUT-121.

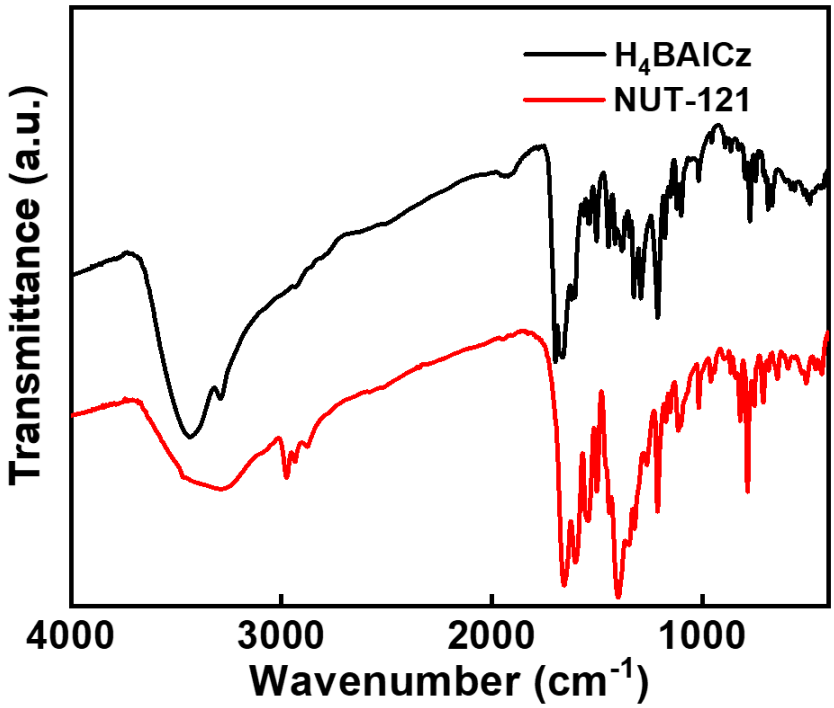

Fig. S5 FT-IR spectra of H_4BAICz and NUT-121 recorded over the range of 4000-400 cm^{-1}.

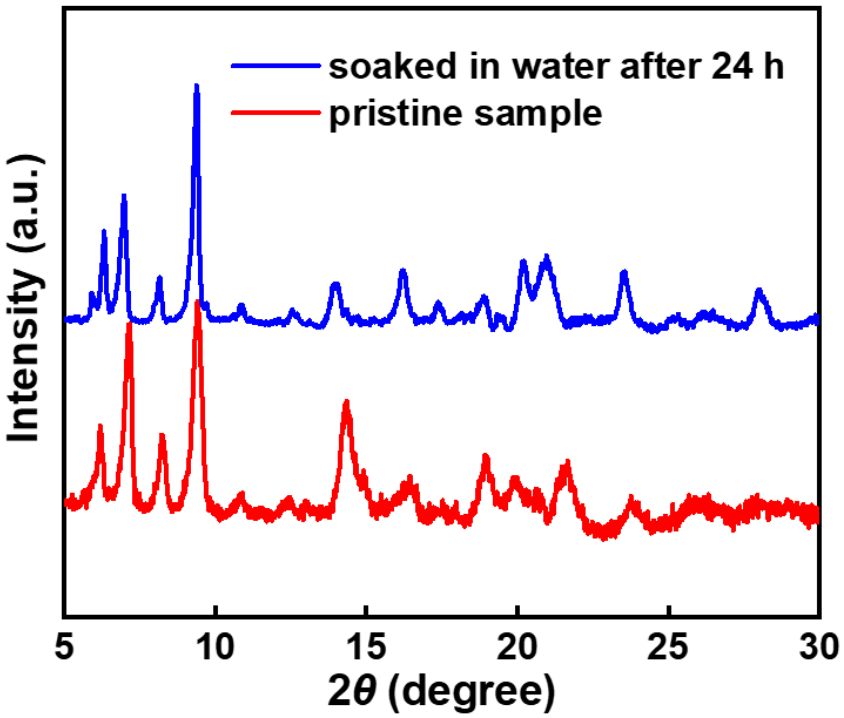

Fig. S6 PXRD patterns of NUT-121 soaked in water after 24 h.

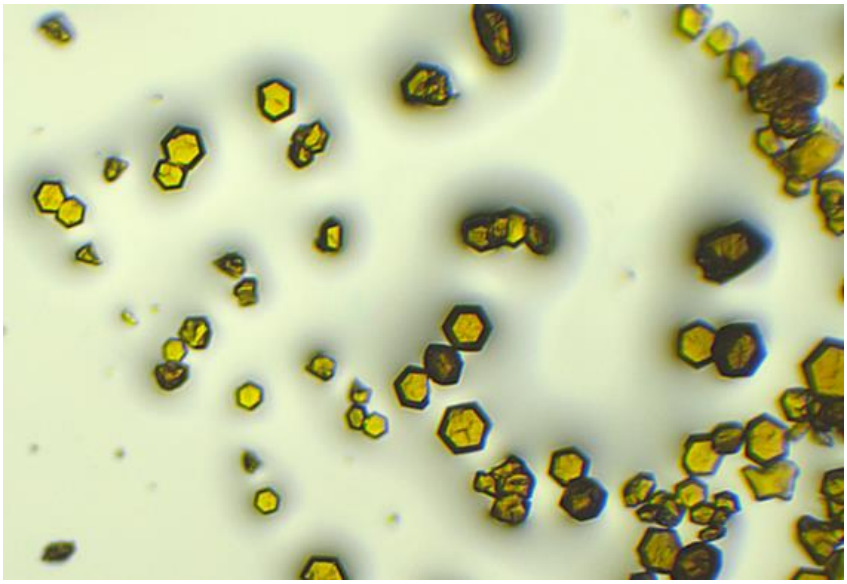

Fig. S7 The yellow hexagonal shaped single crystals of NUT-121.

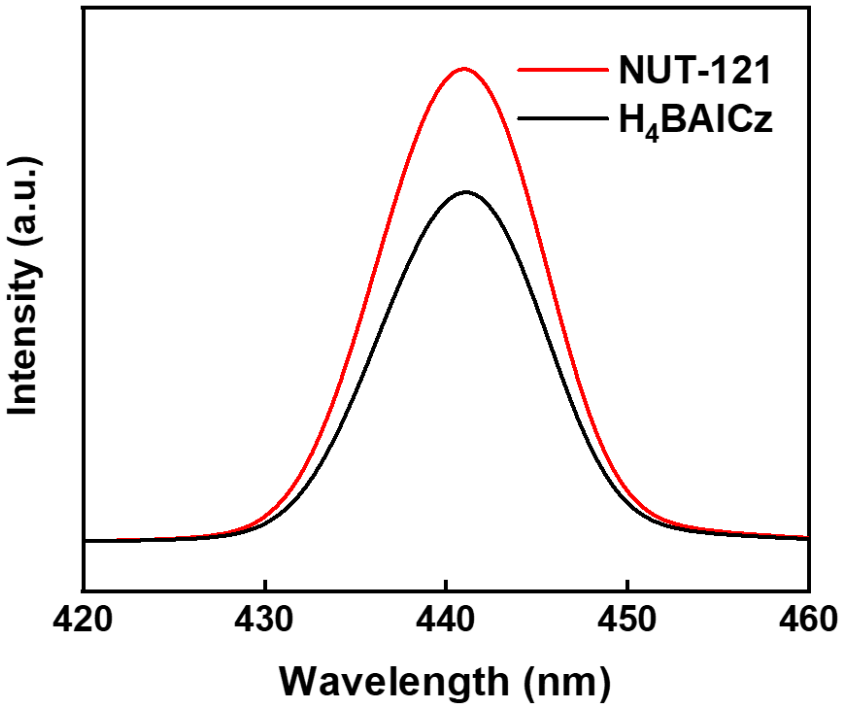

Fig. S8 The fluorescence properties of H_4BAICz and NUT-121.

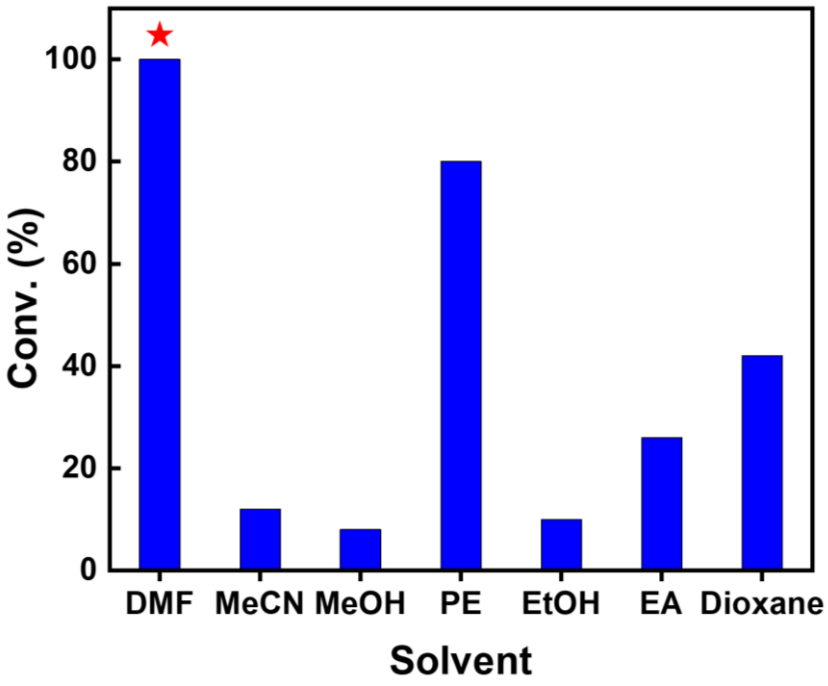

Fig. S9 The solvent influence on the coupling of benzylamine over NUT-121.

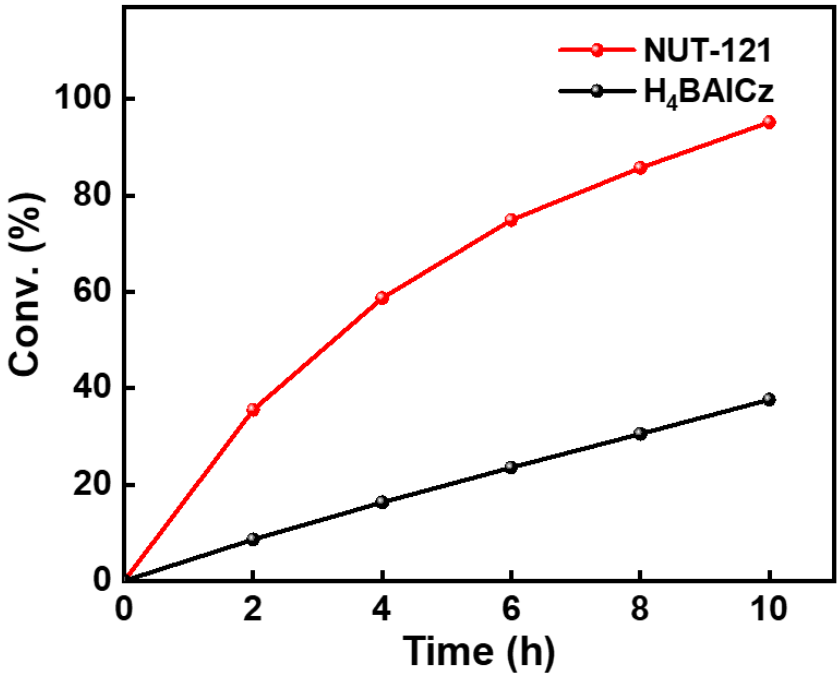

Fig. S10 Conversion of benzylamine in the presence of NUT-121 and H_4BAICz.

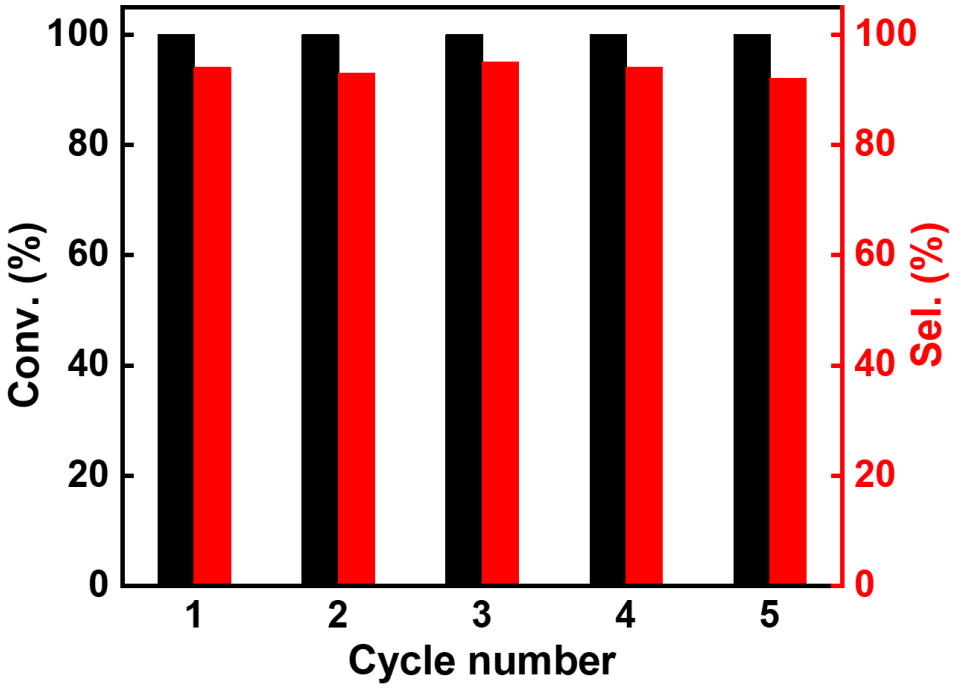

Fig. S11 Reusability of NUT-121 over 5 cycles of photocatalysis of amines to imines.

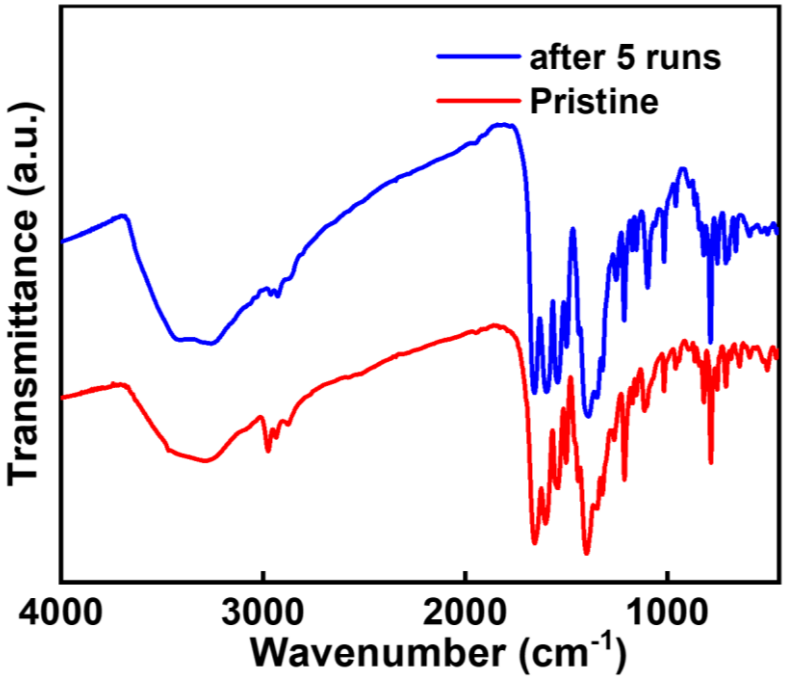

Fig. S12 FT-IR of NUT-121 after 5 runs.

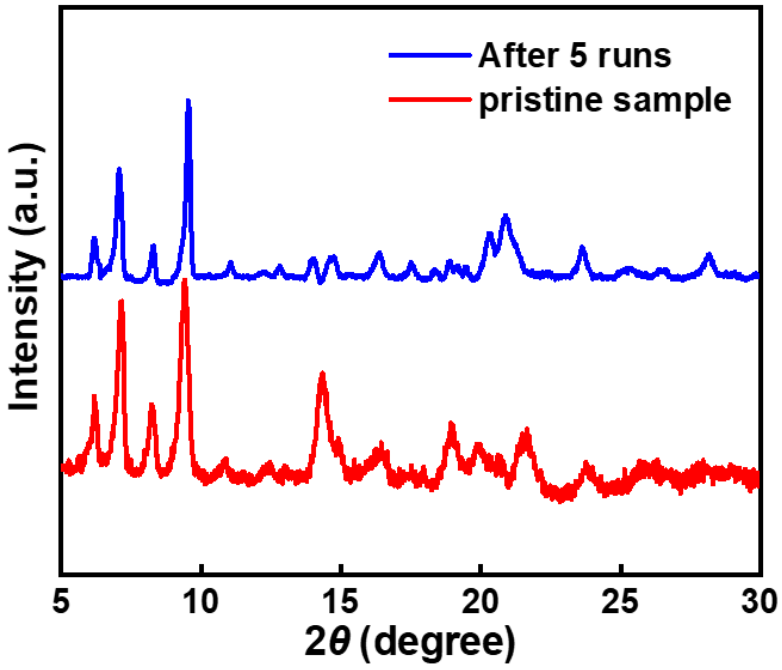

Fig. S13 PXRD of NUT-121 after 5 runs.

Table S1. Crystal Data and Structure Refinement for H_4BAICz and NUT-121

Complex	H_4BAICz	NUT-121
CCDC	2506010	2506011
formula	$C_{34}H_{20}N_2O_8\cdot(H_2O)_{12}$	$C_{68}H_{32}N_4O_{17}Zn_5$
formula weight	800.71	1503.82
crystal system	monoclinic	trigonal
space group	P 2_1/c	P 3_1
a /Å	13.6842(14)	14.4383(5)
b /Å	18.427(2)	14.4383(5)
c /Å	8.4602(7)	43.425(2)
α **/ °**	90	90
β **/ °**	99.016(3)	90
γ **/ °**	90	120
V **/Å^3**	2107.0(4)	7839.8(7)
Z	2	3
Temperature /K	200	193
D**calc /g cm^{-3}**	0.812	0.956
F **(000)**	844	2262
restrain/parameters	0/175	729/746
Goodness-of-fit on F^2	1.019	0.995
R1, wR2 [I > 2σ(I)]	0.1534, 0.3181	0.0970, 0.2525
R1, wR2 (all data)	0.2055, 0.3532	0.2245, 0.3511

[a] $R_1 = \sum(|F_0| - |F_C|) / \sum|F_0|$. $wR_2 = [\sum w(F_0^2 - F_C^2)^2 / \sum w(F_0^2)^2]^{0.5}$

Table S2. Selected bond lengths (Å) and angles (º) for NUT-121

Zn(1)-O(1)	1.90(2)	Zn(1)-O(7)	1.78(2)
Zn(1)-O(13)	1.87(2)	Zn(1)-O(18)	2.26(5)
Zn(2)-O(2)	1.76(3)	Zn(2)-O(15)	2.04(3)
Zn(2)-O(17)	1.71(5)	Zn(2)-O(18)	1.73(5)
Zn(3)-O(4)	1.994(18)	Zn(3)-O(10)	2.09(2)
Zn(3)-O(16)	1.92(2)	Zn(3)-O(17)	2.07(5)
Zn(4)-O(3)	1.916(16)	Zn(4)-O(5)	1.97(2)
Zn(4)-O(9)	1.79(2)	Zn(4)-O(17)	2.13(5)
Zn(5)-O(6)	1.87(3)	Zn(5)-O(12)	2.17(3)
Zn(5)-O(17)	1.62(5)	Zn(5)-O(18)	1.85(5)
Zn(6)-O(8)	2.10(2)	Zn(6)-O(11)	1.83(2)
Zn(6)-O(14)	1.92(2)	Zn(6)-O(18)	2.17(4)
O(1) -Zn(1)-O(18)	109.7(13)	O(7) -Zn(1)-O(1)	104.1(9)
O(7) -Zn(1)-O(13)	103.5(9)	O(7) -Zn(1)-O(18)	85.6(11)
O(13) -Zn(1)-O(1)	141.2(10)	O(13) -Zn(1)-O(18)	99.1(13)
O(2) -Zn(2)-O(15)	124.1(12)	O(17) -Zn(2)-O(2)	118(2)
O(17) -Zn(2)-O(15)	105.5(13)	O(17) -Zn(2)-O(18)	88.5(15)
O(18) -Zn(2)-O(2)	118.0(19)	O(18) -Zn(2)-O(15)	95.9(16)
O(4) -Zn(3)-O(10)	109.2(8)	O(4) -Zn(3)-O(17)	101.9(10)
O(16) -Zn(3)-O(4)	113.7(8)	O(16) -Zn(3)-O(10)	117.6(9)
O(16) -Zn(3)-O(17)	111.2(16)	O(17) -Zn(3)-O(10)	101.5(12)
O(3) -Zn(4)-O(5)	109.4(8)	O(3) -Zn(4)-O(17)	86.2(9)
O(5) -Zn(4)-O(17)	109.0(15)	O(9) -Zn(4)-O(3)	130.6(9)
O(9) -Zn(4)-O(5)	114.3(9)	O(1) -Zn(4)-O(1)	100.2(11)
O(6) -Zn(5)-O(12)	127.9(12)	O(17) -Zn(5)-O(6)	127.0(15)
O(17) -Zn(5)-O(12)	96.6(14)	O(17) -Zn(5)-O(18)	87.3(15)
O(18) -Zn(5)-O(6)	112(2)	O(18) -Zn(5)-O(12)	95.6(14)
O(8) -Zn(6)-O(18)	98.2(12)	O(11) -Zn(6)-O(8)	130.7(10)
O(11) -Zn(6)-O(14)	104.2(10)	O(11) -Zn(6)-O(18)	109.6(15)
O(14) -Zn(6)-O(8)	110.5(7)	O(14) -Zn(6)-O(18)	99.3(13)

Symmetry transformations used to generate equivalent atoms: *#1 -x+1,y-1/2,-z+1/2； #2 -x+1,-y+1,-z； #3 -x+1, y+1/2, -z+1/2.*

Table S3. Comparison for the photocatalytic performance of NUT-121 with reported porous materials

Catalyst	Conditions	*t* (h)	Conv. (%)	Sel. (%)	Refs.
Por-sp^2-COF	Red light, Air	0.25	94	99	1
NMNs	Xe lamp, O_2	4	91.6	99.9	2
HNU-64	Xe lamp, O_2	7	93.2	99	3
SAD	Xe lamp, Air	6	85	99	4
TpBD-COF	Violet LEDs, Air	2.7	90	96	5
In-PQTB	White LED, O_2,	24	81	87	6
UiO-68-BT	Blue LED, Air	0.5	96	99	7
ETBC-por COF	Xe lamp, O_2	12	99	96	8
NUT-121	Blue LED, Air	10	100	94	This work

References

1. J. L. Shi, R. Chen, H. Hao, C. Wang and X. Lang, *Angew. Chem. Int. Ed.*, 2020, **59**, 9088-9093.
2. T. Wu, Y. Shi, Z. Wang, C. Liu, J. Bi, Y. Yu and L. Wu, *ACS Appl. Mater. Interfaces*, 2021, **13**, 61286-61295.
3. G. Che, W. Yang, C. Wang, M. Li, X. Li and Q. Pan, *Inorg. Chem.*, 2022, **61**, 12301-12307.
4. S. Mandal, B. Kommula and S. Bhattacharyya, *ACS Sustainable Chem. Eng.*, 2023, **11**, 14921-14931.
5. K. Xiong, Y. Wang, F. Zhang, X. Li and X. Lang, *Appl. Catal. B: Environ.*, 2023, **322**, 122135.
6. Z. Chen, L. Cao, A. Liu, P. Liu, Y. Chen, J. Yan and B. Li, *J. Mater. Chem. A*, 2024, **12**, 30582-30590.
7. B. Zeng, Y. Wang, F. Huang, K. Xiong, K. Zhang and X. Lang, *Catal. Sci. Technol.*, 2024, **14**, 2838-2847
8. H. Shan, Z. Zhang, Y. Jiang, D. Cai, P. Qin and J. Baeyens, *Sep. Purif. Technol.*, 2025, **363,** 132102.